AGU PUBLICATIONS

Geochemistry, Geophysics, Geosystems

RESEARCH ARTICLE
10.1002/2016GC006711

Halogen variations through the quenched margin of a MORB lava: Evidence for direct assimilation of seawater during eruption

Michael W. Broadley[1,2], Ray. Burgess[2], Hidenori. Kumagai[3,4], Natalie M. Curran[2], and Chris J. Ballentine[5]

[1]Centre de Recherches Pétrographiques et Géochimiques, Vandoeuvre-Lès-Nancy Cedex, France, [2]School of Earth Atmospheric and Environmental Science, University of Manchester, Manchester, UK, [3]IFREE, Japan Agency for Marine—Earth Science and Technology, Yokosuka, Japan, [4]Now at R&D Center for Submarine Resources, Japan Agency for Marine—Earth Science and Technology, Nankoku, Japan, [5]Department of Earth Sciences, University of Oxford, Oxford, UK

Key Points:
- Halogens within submarine basaltic glass are susceptible to being overprinted from the surrounding marine environment
- Up to 70% of the Cl in the quenched basaltic glass margin was found to be derived from the assimilation of a Cl-rich brine during eruption
- Alteration of basaltic glass in direct contact with seawater can introduce an I-rich component and overprint the original MORB I/Cl ratio

Supporting Information:
- Supporting Information S1

Correspondence to:
M. W. Broadley,
michaelwbroadley@gmail.com

Citation:
Broadley, M. W., R. Burgess, H. Kumagai, N. M. Curran, and C. J. Ballentine (2017), Halogen variations through the quenched margin of a MORB lava: Evidence for direct assimilation of seawater during eruption, *Geochem. Geophys. Geosyst.*, *18*, 2413–2428, doi:10.1002/2016GC006711.

Received 2 NOV 2016
Accepted 16 MAY 2017
Accepted article online 22 MAY 2017
Published online 3 JUL 2017

Abstract Halogens and noble gases within submarine basaltic glasses are critical tracers of interactions between the surface volatile reservoirs and the mantle. However, as the halogens and noble gases are concentrated within seawater, sediments, and the oceanic crust this makes the original volatile signature of submarine basaltic lavas susceptible to geochemical overprinting. This study combines halogen (Cl, Br, and I), noble gas, and K concentrations within a single submarine basaltic quenched margin to quantify the amount of seawater assimilation during eruption, and to further elucidate the mechanisms of overprinting. The outer sections of the glass rim are enriched in Cl compared to the interior of the margin, which maintains mantle-like Br/Cl, I/Cl, and K/Cl ratios. Low Br/Cl and K/Cl in the outer sections of the basaltic glass margin indicate that the Cl enrichment in the outer glass is derived from the assimilation of a saline brine component with up to 70% of the Cl within the glass being derived from brine assimilation. Atmospheric noble gas contamination is decoupled from halogen contamination with contaminated outer sections maintaining MORB-like $^{40}Ar/^{36}Ar$, suggesting seawater-derived brine assimilation during eruption is not the dominant source of atmospheric noble gases in submarine basalts. Volatile heterogeneities in submarine basalts introduced during and after eruption, as we have shown in this study, have the potential to expand the range of mantle halogen compositions and only by better understanding these heterogeneities can the Br/Cl and I/Cl variance in mantle derived samples are determined accurately.

1. Introduction

Volatiles such as the halogens (Cl, Br, and I) and noble gases (He, Ne, Ar, Kr, and Xe) provide powerful tracers for the distribution of primordial and recycled volatile components within the mantle [*Graham*, 2002; *Holland and Ballentine*, 2006; *Kendrick et al*., 2012a]. The analysis of halogen and noble gases in mantle derived samples has revealed that the mantle is heterogeneous due to inefficient mixing and the continuous addition of crustal material and atmospheric/marine volatiles through subduction [*Kendrick et al*., 2012a; *Mukhopadhyay*, 2012; *Pepin and Porcelli*, 2002].

The noble gas composition of the Earth's upper mantle has been determined almost exclusively from the analysis of quenched glass from mid-ocean ridge basalts (MORB). Gases trapped in vesicles of submarine basaltic glass are considered to most faithfully preserve the original magmatic noble gas signature and therefore the analysis of gases released from vesicles within basaltic glass represents the best means to determine the primary noble gas composition of the source mantle [*Burnard et al*., 1994]. Submarine basaltic glass is also considered to faithfully preserve the original magmatic halogen signature due to the high solubility of halogens in the melt when erupted in seawater at high pressure and depth [*Schilling et al*., 1980].

In spite of their widespread application in mantle volatile studies however, submarine basaltic glass invariably contains an atmospheric noble gas component [*Burnard et al*., 2004; *Kent et al*., 1999; *Patterson et al*., 1990]. Atmospheric contamination can be introduced to the submarine glass through subduction recycling directly into the mantle source, the assimilation of seawater during eruption or through sample handling [*Ballentine and Barfod*, 2000; *Patterson et al*., 1990]. In order to minimize atmospheric noble gas contamination, the

outermost glassy rind of submarine basalts is often chosen due to their rapid quench rate and ability to retain magmatic gas-rich vesicles [*Kumagai and Kaneoka*, 1998].

The quenching of basaltic glass upon contact with seawater however, poses a problem for the study of halogens as seawater is many times more enriched in halogens compared to basaltic melts [*Deruelle et al*., 1992; *Jambon et al*., 1995; *Kendrick et al*., 2012a; *le Roux et al*., 2006; *Saal et al*., 2002; *Schilling et al*., 1978]. Any degree of late stage contamination within the glass therefore must be taken into account in order to determine the original mantle volatile signature and, or input from deeper hydrothermal contamination.

If the volatile component within submarine basalts is dominated by the assimilation of seawater-derived fluids and, or sedimentary components during eruption then it could obscure the original chemical composition of the mantle and any preeruptive processes. In order to evaluate the extent of contamination within basaltic glasses this study has analyzed the halogen, K, and noble gas content within seven sections forming a transect through a single basaltic glass margin. The examination of the heavy halogens Cl, Br, and I together with K and previously analyzed H_2O data allows for areas of contamination to be identified and quantified [*Kumagai and Kaneoka*, 1998]. Noble gas data previously published and Ar isotopic analysis conducted in this study will aid in identifying the source of contamination and examine the potential link between the contamination of halogens from seawater-derived fluids and the atmospheric contamination of the noble gases [*Kumagai and Kaneoka*, 1998].

2. Background

Submarine basalts with relatively high Cl concentrations are often thought to have assimilated a Cl-rich component such as seawater or hydrothermally altered crust [*Jambon et al*., 1995; *Kent et al*., 1999; *Michael and Cornell*, 1998; *Pietruszka et al*., 2013; *Schilling et al*., 1980; *Soule et al*., 2006]. The partition coefficient of Cl during melting is similar to K, such that the K/Cl ratio of the uncontaminated basalts will likely represent the original mantle composition [*Michael and Cornell*, 1998]. As the K/Cl ratio does not change during melting and crystal fractionation, variations from the mantle value represents the addition or loss of K or Cl due to nonmagmatic processes [*Michael and Cornell*, 1998; *Kent et al*., 1999]. Lowering the K/Cl ratio from the average mantle value is therefore thought to indicate the addition of seawater, hydrothermal brines or hydrothermally altered crust into the melt as seawater-derived components are enriched in Cl and deficient in K compared to silicate melts [*Kendrick et al*., 2012b; *Kent et al*., 1999; *Michael and Cornell*, 1998].

Comparing the K/Cl ratio of submarine basalts provides a test on whether they contain a seawater-derived component and can be used to quantify the amount of Cl that has been assimilated. Chlorine-rich basalts from the Lau Basin and Galápagos Spreading Centre are estimated to have derived up to 95% of their total Cl from the direct assimilation of hydrothermal brines [*Kendrick et al*., 2013]. Submarine basalt samples with low K/Cl ratios have also been shown to have excess ^{234}U, from the combined assimilation of hydrothermal brines (source of Cl) and hydrothermally altered crust (^{234}U excess) during ascent, indicating assimilation can occur from a variety of sources prior to, during and after eruption [*Pietruszka et al*., 2013].

Less is known about the effects of seawater/brine and hydrothermally altered crust assimilation on the abundances of Br and I in submarine basalts. Submarine basalts with low K/Cl ratios attributed to the assimilation of seawater-derived fluids have been found to have Br/Cl ratios higher than both seawater and uncontaminated MORB glasses [*Kendrick et al*., 2013]. The formation of hydrothermal brines deep within the crust has the potential to fractionate Br and Cl during phase separation as well as through the interaction with surrounding wall rock [*Foustoukos and Seyfried*, 2007; *Kendrick et al*., 2013; *Liebscher et al*., 2006; *Oosting and Von Damm*, 1996]. Therefore, elevated Br/Cl ratios within these samples are thought to have been introduced through the assimilation of hydrothermal brines within the magma chamber. Submarine basalts with Br/Cl outside the range of uncontaminated MORB samples may therefore indicate the presence of an assimilated Cl-rich component.

Iodine, unlike Cl and Br, is predominantly concentrated in biogenic ocean sediments that are characterized by higher than seawater Br/Cl and I/Cl values [*Fehn et al*., 2000, 2003, 2007; *Kastner et al*., 1990; *Maramatsu et al*., 2007; *Martin et al*., 1993]. The eruption of basaltic lava onto the ocean floor has been shown to incorporate a sedimentary-like noble gas component, which has been attributed to the interaction of the lava with fine-grained ocean sediments [*Kumagai and Kaneoka*, 1998]. It is therefore also possible that some of

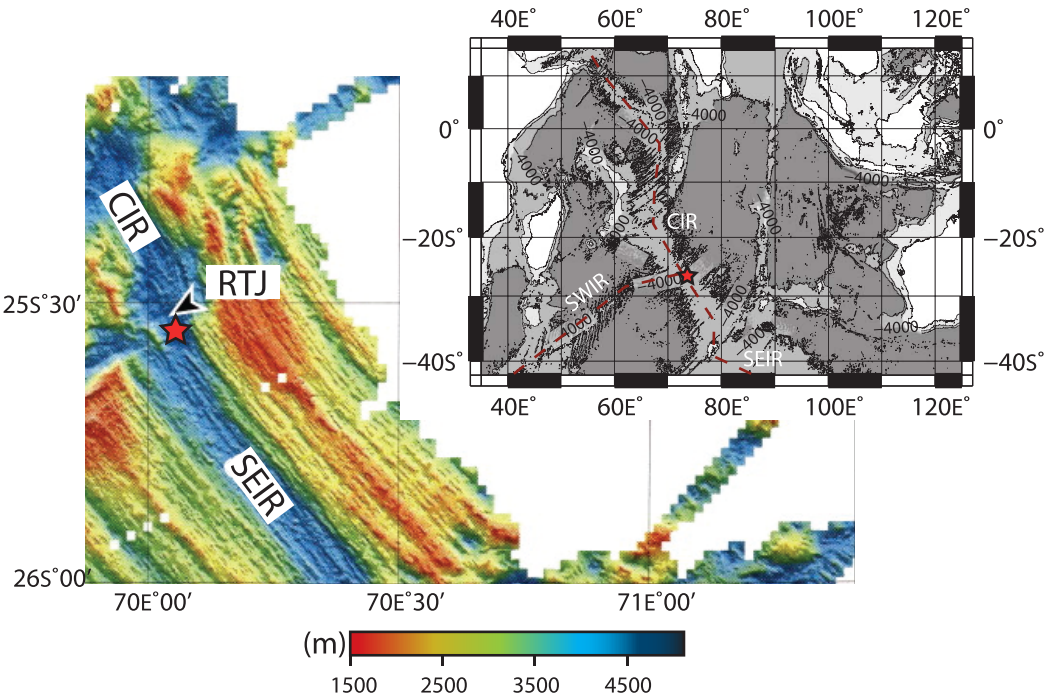

Figure 1. Bathymetric map of the Indian Ocean, showing the sample location (red star) and its position relative to the dominant ridges in the area. The sample was formed in the neovolcanic zone of the Rodriguez Triple Junction (RTJ, 25°35′S 70°04′E), on the boundary between the Central (CIR), Southeast (SEIR) and Southwest (SWIR) Indian Ridges. Figure adapted from *Nakamura et al.* [2007].

the halogens contained within seafloor basalts may also derive directly from the assimilation of sedimentary volatile component in locations with high sedimentation rates.

3. Sample Characteristics

Sample DR25A1b was dredged from the Rodriguez Triple Junction (RTJ) (25°35′S 70°04′E) (Figure 1) at a depth and pressure of 4270 m and 43 Mbar respectively, during the KH93–3 cruise of the R/V Hakuho Maru. The RTJ is the meeting point of three ridge systems; the Central Indian Ridge (CIR, half-spreading rate of 2.7 cm yr^{-1}), the Southeast Indian Ridge (SEIR, 3.0 cm yr^{-1}), and the Southwest Indian Ridge (SWIR, 0.65 cm yr^{-1}). The slow spreading rates of the rifts are generally considered to limit hydrothermal assimilation at depth due to the deeper calculated crystallization depth, although evidence of hydrothermal assimilation in slow spreading ridges does exist indicating spreading rate is not the dominant feature controlling assimilation [*Michael and Cornell*, 1998; *Michael et al*., 2003; *van der Zwan et al*., 2015]. The sampling site of DR25A1b is located at the inner wall of the axial deep in a miniature segment of the RTJ. The sample site was selected due to its proximity to summit of volcanoes that have shown recent igneous activity within the neovolcanic zone of the RTJ [*Kumagai and Kaneoka*, 2005].

The recovered sample represents a quenched margin with a ~1 cm thick convex glass rind overlying a concave crystalline surface from a drained tholeiitic normal MORB (N-MORB) lava flow [*Michard et al*., 1986; *Price et al*., 1986]. The outer section of the chilled margin (#1 to #3) is composed predominantly of glass with some olivine and plagioclase microlites. The inner sections of the chilled margin (#4 to #6) are a mix of glass and crystals with fibrous varioles centred on plagioclase phenocrysts increasing with depth of the section. Section #7 is completely crystalline and dominated by euhedral plagioclase and minor olivine microlites [*Kumagai and Kaneoka*, 1998].

Kumagai and Kaneoka [1998] analyzed noble gases in seven positions across the chilled margin of sample DR25A1b, which revealed evidence for seawater and sedimentary-like noble gas incorporation. The surface of the glass rim has lower $^{40}Ar/^{36}Ar$ ratio (9300) compared to the inner glass sections (17,500), indicating the presence of atmospheric noble gases in the outer glass section (Figure 2). In addition, the deeper

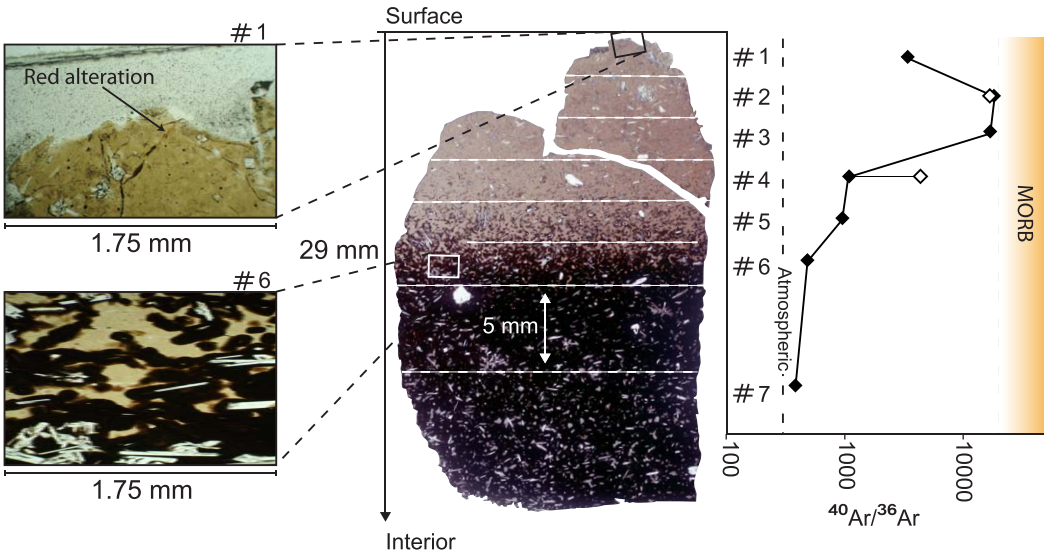

Figure 2. Photomicrograph of DR25A1b, indicating relative positions of each section and magnified images of sections #1 and #6 showing glass and partially crystalline sections, respectively. The $^{40}Ar/^{36}Ar$ ratios of each section from *Kumagai and Kaneoka* [1998], with repeat analysis of sections #2 and #4 (open symbols) from this study are compared to atmospheric and mantle MORB ratios.

crystalline sections of the quenched margin yielded atmospheric-like $^{40}Ar/^{36}Ar$ as well as $^{132}Xe/^{36}Ar$ isotopic ratios identical to oceanic sediments suggesting the lava may have assimilated a noble gas component from fine-grained sediment during eruption [*Kumagai and Kaneoka*, 1998]. The lack of sedimentary Xe signature within the glass was interpreted as evidence that sedimentary addition occurred after the rapid quenching of the glass rim, either from direct incorporation from underlying sediment into the molten interior of the lava flow, or from the subsequent influx of water and adsorption of noble gases with a sedimentary noble gas signature onto grain boundaries. This sample therefore has well documented evidence of seawater interaction within the glass as well as possible sedimentary addition within the crystalline sections permitting the effect of seawater/sedimentary interaction on the halogen signature of submarine basalts to be examined.

4. Methods

The sample was obtained from the previous work by *Kumagai and Kaneoka* [1998]. The chilled margin was sliced into seven sections parallel to the outer most glass rim at 2.5 mm intervals using a microsaw to produce mm sized chips of sample from the glass rim to the crystalline interior of the quenched margin (Figure 2). To ensure full coverage of the 29 mm margin, section #7 was a further 5 mm inward from section #6 and is entirely crystalline. Sections analyzed in this study for halogens were either in the form of powders (#1, #3, #5, #6, and #7) or as whole rock chips (#2 and #4), which were analyzed using identical analytical procedures.

Sufficient material was available from sections #2 and #4 to be cut and polished for sample characterization by back scatter electron imaging (BSE) and electron dispersive spectroscopy. A FEI XL30 Environmental Scanning Electron Microscope-Field Emission Gun (ESEM-FEG) was used to obtain BSE images, and an EDAX Gemini EDS detector operating at 15 kV accelerating voltage was used to obtain X-ray element distribution maps (supporting information figures). The X-ray maps were created using a resolution of 512 × 512 at a magnification of 300–700.

The heavy halogens (Cl, Br, I) and K were measured simultaneously using neutron irradiation-noble gas mass spectrometry (NI-NGMS) [*Böhlke and Irwin*, 1992; *Johnson et al*., 2000; *Kendrick*, 2012; *Merrihue and Turner*, 1966; *Ruzié-Hamilton et al*., 2016]. Samples weighing ~10–50 mg were wrapped in Al foil and sealed in evacuated glass tubes. Each tube contained several Hb3gr hornblende ^{40}Ar–^{39}Ar dating standards as flux monitors as well as several Shallowater meteorite I-Xe dating standards to monitor the production of noble gases from halogens [*Ruzié-Hamilton et al*., 2016].

Samples were irradiated in two batches at the RODEO reactor in Petten, Netherlands, for a total of 24 h. Sections #2, #3, #5, and #7 were irradiated on the 24 July 2012, receiving a fast neutron flux of 1.2×10^{18} cm^{-2}, a thermal flux of 6.3×10^{18} cm^{-2} and with a corresponding J value of 0.006442 ± 0.000011. Sections #1, #4, and #6 were irradiated under the same protocols on the 28 July 2013, receiving a fast neutron flux of 1.2×10^{18} cm^{-2}, a thermal flux of 6.7×10^{18} cm^{-2} and with a corresponding J value of 0.006256 ± 0.000020.

Noble gas proxy isotopes ($^{38}Ar_{Cl}$, $^{80}Kr_{Br}$, $^{128}Xe_{I}$, and $^{39}Ar_{K}$) formed during irradiation were extracted by step heating using a tantalum resistance furnace using three temperature steps of 600, 1400, and 1600°C. Prior to analysis, the furnace was baked in seven cycles up to 1700°C to ensure a low blank was achieved. Air calibrations and blanks were analyzed daily to check the sensitivity and background of the spectrometer, with maximum furnace blank values at 1600°C being 5.08×10^{-9} cm^3 STP ^{40}Ar, 2.92×10^{-13} cm^3 STP ^{84}Kr, and 3.54×10^{-14} STP cm^3 ^{132}Xe. Extracted gases were purified for 5 min on Al-Zr getters at 250°C and were then analyzed using the MS1 noble gas mass spectrometer [*Broadley et al*., 2016; *Burgess et al*., 2002; *Johnson et al*., 2000; *Sumino et al*., 2010]. The analysis of sections #5, #6, and #7 was also repeated in order to monitor the precision of the analysis and ensure section homogeneity. Corrections for blanks and mass bias and several other corrections including atmospheric contributions were applied to the raw data following the procedures in *Ruzie-Hamilton et al*. [2016] giving an external precision of 3% (1σ) for Cl and K, and 7% (1σ) for Br and I determinations.

In addition to the halogen measurements, sufficient material from sections #2 and #4 was available to analyze the Ar isotopes without being irradiated. This ensured that the magmatic $^{40}Ar/^{36}Ar$ signature original reported by *Kumagai and Kaneoka* [1998] was consistent throughout the whole section and small-scale contamination had not introduced variable amounts of atmospheric noble gases. Larger samples (32–33 mg) were analyzed using a more extensive step heating procedure (600, 800, 1000, 1400, and1600°C) in an attempt to resolve atmospheric argon adsorbed on the grain surfaces. Samples were analyzed using the same gas extraction procedure described above, with the exception that only Ar isotopes were measured.

5. Results

5.1. Sample Description and Alteration

Back scattered electron images reveal section #2 is composed mainly of glass interspersed with microlites of plagioclase (<1 mm) and small blebs of metal sulphides (<0.1 mm). The glass section has very few vesicles (much less than 1%) and any vesicles present are <10 μm. X-ray mapping reveals homogeneous and low Cl concentrations in section #2, areas of visible Cl-rich alteration or Cl bearing alteration minerals are not present in this thin section (supporting information Figure S2).

5.2. Halogens and Potassium

Halogens (Cl, Br, and I) and K concentrations for each section of the chilled margin are given in Figure 3 and Table 1. Elemental ratios are given as molar values and errors quoted at two standard deviations. The concentration of Cl, Br, I, and K varies significantly across the chilled margin, with Cl and I especially variable within the glass sections (Figure 4). The average Cl concentration is 30 ppm with variability of sections #1, #3 to #7 ranging from 12 ppm (#6) to 31 ppm (#7). Section #2 is significantly more enriched in Cl relative to the other sections at 66 ppm. Despite the range in Cl concentration, there is no obvious systematic variation, with glass sections having concentrations similar to those in the crystalline interior (Table 1 and Figure 4). Chlorine concentrations of the sections are consistent with previously reported values from N-MORB samples (32–630 ppm; Figure 3) and samples originating from slow spreading ridges, but are much lower than some rare, Cl-rich N-MORB glass shards (4000–7000 ppm) [*Jambon et al*., 1995; *Kendrick et al*., 2013; *Michael and Cornell*, 1998; *Portner et al*., 2014]. Concentrations of K range from 539 ppm in section #2 to 1109 ppm in section #7 (Figure 3). Like the Cl concentrations, there is no systematic variation between the glass and crystalline sections.

Bromine abundances vary between 43 ppb (section #6) and 94 ppb (section #7). No systematic variation in Br concentrations across the sections exists (Figure 4) with no apparent difference between glass and crystalline samples. Iodine concentrations range from 1 ppb (section #2) to 11 ppb (section #1). Overall I

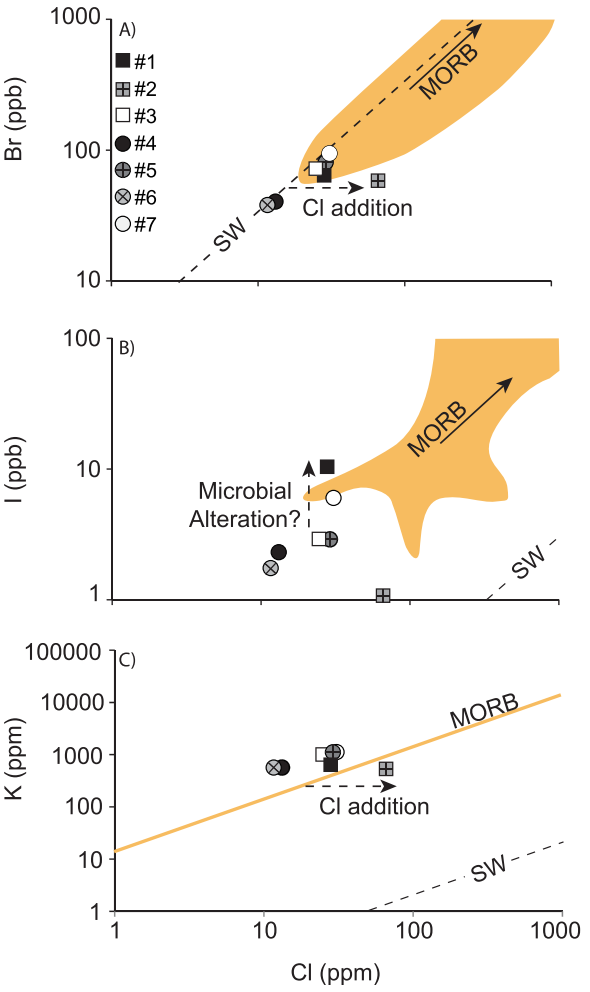

Figure 3. Concentrations of (a) Br, (b) I, and (c) K all relative to Cl are shown for all sections. Square symbols represent glass sections while crystaline sections are represented by circles. All symbols encompass analytical error bars. Samples are plotted against the range of Br/Cl and I/Cl measured in MORB and the global mantle average K/Cl, as well as seawater [*Deruelle et al.*, 1992; *Jambon et al.*, 1995; *Kendrick et al.*, 2012b].

concentrations show little variation expect for section #1 (6 ppb) and #7 (11 ppb) which are enriched relative to the rest of the section (1–3 ppb; Figures 3 and 4). Br and I concentrations within all sections are similar to the range of concentrations reported previously for MORB glass (Br = 60–1900 ppb; I = 2–20 ppb) [*Deruelle et al.*, 1992; *Jambon et al.*, 1995; *Kendrick et al.*, 2013].

There is little variation in Br/Cl, K/Cl, and I/Cl from glass section #3 to the crystalline interior section #7, while sections #1 and #2 exhibit markedly different ratios. The Br/Cl of sections #1 (1.0×10^{-3}) and #2 (0.4×10^{-3}) are significantly lower than the range in sections #3 to #7 ($1.2–1.5 \times 10^{-3}$). The variation in K/Cl is similar to Br/Cl with both sections #1 (20.5 ± 0.5) and #2 (7.4 ± 0.1) being lower than sections #3 to #7 (36.0–46.5). The I/Cl ratios of sections #1 (103.1×10^{-5}) and #2 (0.5×10^{-5}) are also distinct from the range of values in sections #3 to #7 ($1.6–3.0 \times 10^{-5}$) but do not follow the same pattern as Br/Cl and K/Cl, with section #1 having the highest and section #2 the lowest I/Cl of all sections.

The Br/Cl of sections #3 to #7 is similar to the range of values previously reported for uncontaminated MORB samples ($1.2–1.3 \times 10^{-3}$), while sections #1 and #2 are an order of magnitude lower. The I/Cl in sections #3 to #7 ranges from MORB-like ($1.6–3.0 \times 10^{-5}$) to slightly elevated values, while section #1 is significantly enriched and section #2 is significantly depleted relative to MORB [*Kendrick et al.*, 2012b, 2013]. The K/Cl ratios of sections #2 to #7 are higher, while the K/Cl of section #1 is lower than the global MORB average (~14) but all sections are within the range previously determined for contamination free, Cl-poor N-MORB [*Bonifacie et al.*, 2008; *Kendrick et al.*, 2012b]. In summary, the Br/Cl, I/Cl, and K/Cl of samples #1 and #2 are consistently different from the rest of the sample (Figure 4).

5.3. Argon

Blank corrected $^{40}Ar/^{36}Ar$ ratios from the total gas release of unirradiated chips #2 and #4 are $16,835 \pm 1627$ and 4208 ± 148, respectively (Figure 2). The lower $^{40}Ar/^{36}Ar$ value of section #4 suggests the degree of air contamination is greater within the partially crystalline sample compared to the glass sample #2. The $^{40}Ar/^{36}Ar$ ratio of #2 is within the variation of MORB source mantle, with MORB $^{40}Ar/^{36}Ar$ heterogeneity attributed to variable amount of recycled atmospheric Ar [*Parai et al.*, 2012]. Further atmospheric Ar may be added through a small degree of surficial air contamination, introduced during sample handling [*Ballentine and Barfod*, 2000]. The $^{40}Ar/^{36}Ar$ ratios from sections #2 are consistent with the maximum ratio determined previously ($17,500 \pm 5600$) while section #4 is higher than previously determined (1213 ± 19) which may be factor of heterogeneity introduced from the increased crystallinity. The higher and more consistent $^{40}Ar/^{36}Ar$ ratio in section #2 confirms that the magmatic noble gas signature is best preserved within the glass rind of the chilled margin [*Kumagai and Kaneoka*, 1998].

Table 1. Halogen and K Data From 1400°C Heating Step of Each Section, Uncertainty is 2σ

Section No.	$^{40}Ar/^{36}Ar$	H_2O[a] (wt %)	Mass (g)	Cl (ppm)	Br (ppb)	I (ppb)	K (ppm)	Br/Cl ($\times10^{-3}$)	I/Cl ($\times10^{-6}$)	K/Cl	H_2O/Cl
#1	3390 ± 370	0.17 ± 0.03	0.003	28.1 ± 0.7	63.9 ± 0.8	10.4 ± 0.3	633.3 ± 3.4	1.01 ± 0.03	103.1 ± 3.7	20.5 ± 0.5	60.5 ± 10.8
#2	17500 ± 930 (16,835 ± 1627)[b]	0.17 ± 0.05	0.010	66.1 ± 0.1	58.1 ± 0.7	1.0 ± 0.1	539.1 ± 1.7	0.39 ± 0.11	4.5 ± 0.4	7.4 ± 0.1	25.7 ± 7.6
#3	17,100 ± 100	0.15 ± 0.03	0.018	24.8 ± 0.3	71.9 ± 0.5	2.9 ± 0.1	997.7 ± 3.1	1.29 ± 0.04	32.5 ± 0.9	40.2 ± 0.9	60.4 ± 12.1
Bulk Glass[d]	12,663 ± 466	0.16 ± 0.02		39.7 ± 0.3	64.6 ± 0.4	4.8 ± 0.1	723.3 ± 1.4	0.90 ± 0.04	46.7 ± 1.3	22.7 ± 0.4	48.9 ± 6.0
#4	1065 ± 18 (4208 ± 148)[b]	0.16 ± 0.03	0.008	13.2 ± 0.2	40.2 ± 0.5	2.3 ± 0.1	565.6 ± 5.4	1.36 ± 0.02	48.7 ± 1.7	38.9 ± 0.7	121.3 ± 22.8
#5	809 ± 19	0.16 ± 0.03	0.012	29.0 ± 0.7	80.4 ± 0.9	2.9 ± 0.1	1108.0 ± 6.1	1.23 ± 0.03	27.9 ± 1.2	38.2 ± 0.8	55.1 ± 10.4
	(reanalysis)[c]		*0.008*	*28.8 ± 7.6*	*79.9 ± 0.6*	*3.2 ± 0.1*	*1106 ± 10.36*	*1.23 ± 0.03*	*30.8 ± 8.2*	*35.4 ± 0.6*	*55.6 ± 18.0*
#6	499.8 ± 8	0.17 ± 0.03	0.020	11.6 ± 0.2	37.9 ± 0.3	1.7 ± 0.1	568.8 ± 6.2	1.45 ± 0.02	41.8 ± 1.6	44.4 ± 0.8	140.1 ± 25.9
	(reanalysis)[c]		*0.010*	*11.3 ±0.2*	*35.6 ± 2.7*	*2.4 ± 0.4*	*566.5 ± 2.0*	*1.40 ± 0.11*	*60.5 ± 10.6*	*45.6 ± 0.8*	*150.6 ± 25.7*
#7	387 ± 7	0.23 ± 0.03	0.010	30.8 ± 1.0	94.1 ± 4.9	6.0 ± 0.2	1109.3 ± 30.9	1.36 ± 0.08	54.4 ± 2.3	36.0 ± 1.4	74.7 ± 10.1
	(reanalysis)[c]		*0.009*	*27.3 ± 1.1*	*93.0 ± 0.7*	*5.2 ± 0.2*	*554.6 ± 144.8*	*1.52 ± 0.65*	*53.4 ± 2.8*	*18.46 ± 4.8*	*80.7 ± 10.7*
Bulk Sample[d]	3894 ± 136	0.17 ± 0.08		29.0 ± 0.3	63.5 ± 1.1	4.0 ± 0.1	788.5 ± 6.2	1.15 ± 0.04	47.4 ± 2.4	39.8 ± 0.4	78.4 ± 6.9
Interior[d]	3972 ± 30	0.17 ± 0.03		21.8 ± 0.3	64.4 ± 1.1	3.3 ± 0.1	869.4 ± 6.1	1.33 ± 0.03	44.8 ± 2.2	32.4 ± 0.4	92.5 ± 9.3
MORB[e]	44,000							1.31 ± 0.28	17.5 ± 8.7	13 ± 4	
Seawater[e]	295.5			19,400	65,877	58	380	1.50	0.86	0.02	50

[a]H_2O concentrations are from *Kumagai and Kaneoka* [1998].
[b]Brackets represent the $^{40}Ar/^{36}Ar$ values determined from unirradiated samples.
[c]Values in italics are reanalyzed samples.
[d]Average values are given for the glass (#1 to #3), the interior sections (#3 to #7) and the whole sample (#1 to #7).
[e]MORB and seawater data from *Graham* [2002] and *Kendrick et al.* [2012b, 2013a].

6. Discussion

6.1. Evidence of Interaction With the Surrounding Marine Environment

The outer glass sections #1 and #2 are enriched in Cl and have different Br/Cl, I/Cl, and K/Cl compared to the interior sections (Figure 4). The Cl enrichment and lower K/Cl in these sections indicates the possible addition of a Cl-rich component into the outer glass margin. As potassium and chlorine have similar compatibilities during melting and fractionation, the K/Cl ratio can therefore exclude Cl variations due to magmatic processes and makes for a sensitive tracer of contamination from Cl-rich seawater and seawater-derived brines [*Kent et al.*, 2002; *Michael and Cornell*, 1998]. The lower K/Cl in sections #1 and #2 indicates that the outer glass sections may have assimilated one of these Cl-rich components.

The variability of Br/Cl and I/Cl across the sections also indicates that sections #1 and #2 have a potentially distinct source of Br and I when compared to the interior sections and the average MORB reservoir (Figure 5). The enriched I/Cl in section #1 cannot be a result of the direct mixing with seawater as the section does not lie on mantle-seawater mixing line (Figure 6). Section #1 originated from the first 2.5 mm of the glass margin, which would have been in continuous contact with surrounding marine environment since its eruption. The alteration of basaltic glass in contact with seawater has been postulated as a potential source of high I/Cl within submarine basaltic glasses [*Kendrick et al.*, 2012b]. The alteration of glass to palagonite which is enriched in I compared to MORB glass is one potential source of the high I/Cl in section #1. Microbial alteration of submarine basaltic glass may also introduce biophilic I, with alteration known to occur on the surface of the basaltic glass almost immediately after eruption [*Templeton et al.*, 2005]. The entrainment of seawater and nutrient-rich hydrothermal fluids into rapidly cooling lava can support conditions for microbial communities to develop and microbial mats up to several meters thick have been discovered at so called "snowblower" events where microbial flocculent emerges from the seafloor covering newly erupted lava flows [*Crowell et al.*, 2008]. These microbial processes may be a contributing factor for the introduction of I in to submarine basaltic glass.

While there is no petrographic evidence of palogonitization features such as, layers of translucent, crystal free "gel-palagonite" or fibrous anisotropic "fibro-palagonite" both with yellow to brown coloration within the glass section small-scale alteration cannot be ruled out as the source of high I/Cl in glass section #1 [*Stroncik and Schmincke*, 2002]. As palagonitization and microbial alteration only affects glass which is in direct contact with seawater such as the surface of the submarine glass margins or along cracks and fractures the high I/Cl appears limited to section #1 which has been in continuous contact with the surrounding seawater (Figure 2). The alteration of basaltic glass from contact with seawater is also likely to introduce seawater-derived atmospheric Ar which could explain the lower $^{40}Ar/^{36}Ar$ ratio within section #1 (Figure 2).

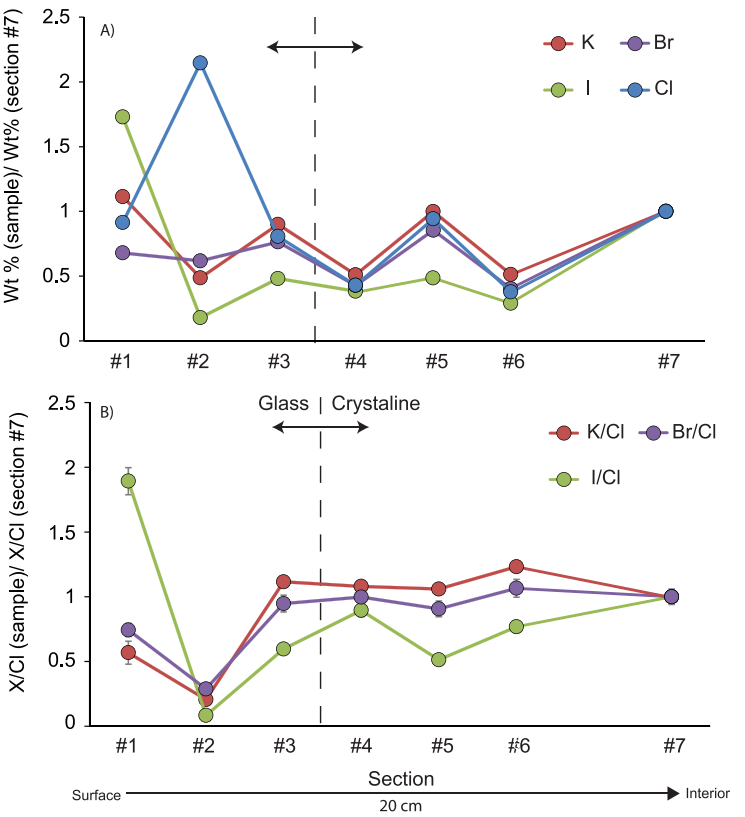

Figure 4. (a) Variations of Cl, Br, I, and K in the chilled margin transect at 2.5 mm intervals from the glass surface (#1) to the crystalline interior (#7). (b) Variations in K/Cl, Br/Cl, and I/Cl along the same transect. All concentrations are normalized to section #7. Data symbols encompass 2σ error bars.

It is therefore considered that the high I/Cl and the low $^{40}Ar/^{36}Ar$ ratio of section #1 is most likely through the alteration of the glass on the surface of the quenched glass margin. Overall the geochemical evidence for alteration is minor within this sample, recording only the first stage of alteration (microbial and palagontization) from the interaction between the glass surface of the lava and surrounding seawater at ambient temperatures.

Section #2, unlike section #1, has an I/Cl ratios which lies below, yet close to the mixing line defined between the average value of sections #3 to #7 and seawater suggesting the assimilated component has a seawater-like I/Cl ratio (Figure 6). Although the I/Cl ratio of section #2 plots close to the mixing line between mantle and seawater end-members, this is not true of the Br/Cl ratio (Figure 6). The Br/Cl ratios of both section #1 and #2 are considerably lower (almost 4 times lower for #2) than the seawater value. H_2O/Cl and K/Cl in sections #1 and #2 are also lower than sections considered to be free from contamination (#3 to #7) and seawater, suggesting these sections have assimilated a Cl-rich component that does not have a seawater-like composition.

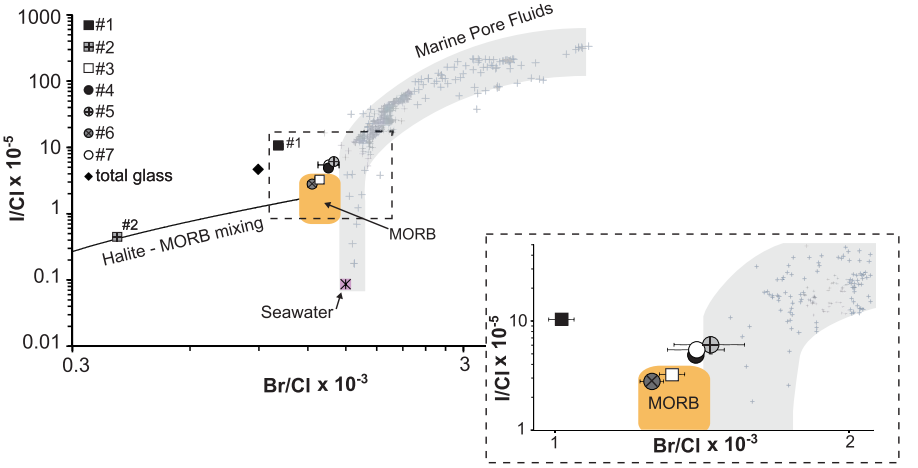

Figure 5. Log-log plot of Br/Cl versus I/Cl for all sections through the chilled margin. Expanded view shows variation of samples within the MORB field. "Total glass" average of glass bearing samples #1 to #3 (Table 1). Reference values are shown for seawater, MORB [*Kendrick et al.*, 2012a] and marine pore fluids/brines [*Fehn et al.*, 2000, 2003; 2007a, 2007b; *Kastner et al.*,1990; *Muramatsu et al.*, 2001, 2007; *Martin et al.*, 1993]. Sections #3 to #7 plot close to MORB values, while sections #1 and #2 suggest some form of seawater contamination. Lines are representative of a mixing line between MORB and halite. Analytical uncertainties are 2σ.

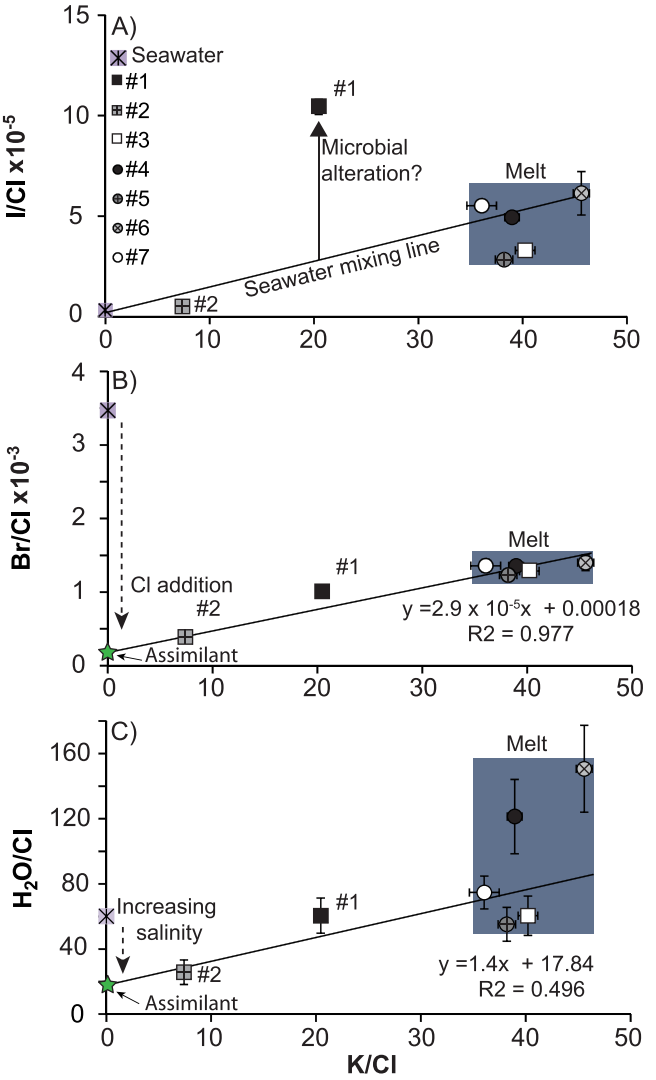

Figure 6. Br/Cl, I/Cl H_2O/Cl of all sections are plotted relative to K/Cl ratio (H_2O data are from *Kumagai and Kaneoka* [1998], given in Table 1). (a) I/Cl versus K/Cl of sections #1 to #7. Mixing line between sections #3 to #7 (average melt composition) and the seawater end-member is shown. Section #2 lies close the seawater end-member while section #1 has much higher I/Cl from possible microbial alteration on the surface of the glass. (b) Br/Cl versus K/Cl and (c) H_2O/Cl versus K/Cl. Lines determined by error-weighted linear regression between the average value for sections #3 to #7 and data for sections #1 and #2 are shown, with the potential assimilant (green star) determined at the intercept.

Potential pathways for the introduction of a Cl-rich component include, the assimilation of hydrothermal brines and, or altered crust, and long-term alteration of the glass in contact with seawater. Chlorine enrichment from hydrothermal processes within the submarine volcanic system is thought to readily introduce Cl-rich components into submarine magmas [*Kendrick et al*., 2013; *Kent et al*., 1999; *Michael and Schilling*, 1989; *van der Zwan et al*., 2015]. Hydrothermal boiling and the formation of brines can occur in the oceanic crust through the interaction with circulating seawater and, or on the seafloor during eruption which could be the source of Cl enrichment within the glass rim. Furthermore, hydrothermal boiling of seawater leads to the partitioning of the noble gases into the vapor phase relative to the gas poor brine. Section #2 has retained a magmatic $^{40}Ar/^{36}Ar$ signature (16,800) similar to the uncontaminated section #3 (17,100) indicating that the assimilant that introduced the Cl-rich component did not introduce significant amounts of atmospheric noble gases associated with seawater (Figure 2). The incorporation of brines prior to or during eruption could be capable of generating the Cl enrichment within glass rim, while maintaining their original magmatic noble gas signature (Figure 6) [*Kendrick et al*., 2013; *Perfit et al*., 2003].

Long-term alteration of the basaltic glass can also introduce Cl into basaltic glass samples through the precipitation and, or incorporation of Cl-rich minerals. Some alteration minerals such as amphibole have similar Br/Cl and I/Cl ratios as those observed in section #2 [*Kendrick*, 2012a; *Kendrick and Burnard*, 2013; *Chavrit et al*., 2016]. Alteration minerals such as carbonates, clay minerals, and serpentine formed during extended hydrothermal interactions, as well as potential amphibole, epidote, and chlorite formation during metamorphism can impart Cl-rich signatures into the basalt [*Kyser and O'Neil*, 1984].

The alteration of the basaltic glass margin is, however, not considered to be the dominant process for introducing the Cl-rich component. There is no petrographic evidence of alteration minerals present within the glass apart from minor microbial and, or palagonitization on the outer surface of the glass. Furthermore Cl element maps created from two chips of the most contaminated section (#2) do not show any evidence for Cl-rich alteration minerals or Cl-bearing phases being present (supporting information Figure S2).

The halogen ratios within sections #1 and #2 are therefore most likely to be the result of a set of complex interactions between a hydrothermal component such as a brine prior to, or during, eruption resulting in

lower than MORB Br/Cl, as well as continuous microbial alteration in the outer glass resulting higher then MORB I/Cl [*Kendrick et al*., 2013; *Perfit et al*., 2003; *Soule et al*., 2006; *van der Zwan et al*., 2015].

6.2. Composition of the Assimilant

The interaction between saline brines created from hydrothermal boiling and phase separation with the melt in the magma chamber, or during eruption can impart a unique signature on the glass which can be resolved by forming binary mixing lines between the contaminated (#1 and #2) and uncontaminated (#3 to #7) sections to determine the H_2O/Cl and Br/Cl ratios of the assimilant and determine its origin [*Kendrick et al*., 2013; *Kent et al*., 2002].

The H_2O/Cl and the Br/Cl ratios within section #2 are much lower than the seawater value (Figure 6). Low H_2O/Cl ratios within basaltic glasses have been attributed to the assimilation of brines, which have a higher salinity than seawater. Extrapolating the H_2O/Cl and Br/Cl ratios relative to the K/Cl ratios from the original mantle source value (#3 to #7) can estimate the ratios of the assimilant and also the salinity of the assimilant, assuming the K/Cl of the assimilant is similar to the average of modern high temperature deep hydrothermal brines (0.1 ± 0.09) [*Böhlke and Irwin*, 1992; *Thompson and Fournier*, 1988, Figure 6]. The average K/Cl (39.8 ± 0.4), H_2O/Cl (92.5 ± 9.3), and Br/Cl ($1.38 \pm 0.15 \times 10^{-3}$) ratios of sections #3 to #7 are used to define the original melt composition. Extrapolated H_2O/Cl and Br/Cl ratio of the assimilant are 17.8 ± 16.3 and $1.83 \pm 0.30 \times 10^{-4}$, respectively. The low H_2O/Cl of the assimilant compared to seawater (50) indicates the assimilant has a higher salinity (9.8%) than pure seawater (3.5%) confirming that the assimilant is most likely a high salinity brine component. The large error associated with H_2O/Cl ratio of the assimilant is due in part to the large variation of H_2O/Cl ratios within the sections used to define the original composition of the melt and the limited number of sections which define the linear regression and the intercept.

Experimental results suggest that the behavior of Br during phase separation and the formation of hydrothermal brines is dependent on the surrounding environmental conditions, resulting in the modification of the original seawater Br/Cl ratio [*Foustoukos and Seyfried*, 2007]. During phase separation Br is preferentially incorporated into the vapor phase [*Foustoukos and Seyfried*, 2007]. The fractionation of Br in to the vapor phase can be further enhanced by a "salting-out" effect producing Br/Cl ratios lower than seawater within the highly saline brines [*Stoessel and Carpenter*, 1986; *Foustoukos and Seyfried*, 2007]. Previous studies of basalts that exhibit evidence of brine assimilation suggest they also have assimilated saline brines with low H_2O/Cl but high Br/Cl ratios, formed through the interaction with amphibole within the crust [*Berndt and Seyfried*, 1990; *le Roux et al*., 2006; *Kendrick et al*., 2013; *van der Zwan et al*., 2015]. The Br/Cl of the assimilant within sections #1 and #2 ($1.38 \pm 0.30 \times 10^{-4}$) is lower than brines present in previously analyzed submarine basaltic glasses (4.0×10^{-3}), but is within the range of brines measured at hydrothermal vents ($0.6–1.7 \times 10^{-3}$) [*Butterfield et al*., 1994; *Kendrick et al*., 2013; *Oosting and Von Damm*, 1996].

Evidence of brine assimilation within the sample is restricted to the outer glass margin and is not pervasive throughout the whole sample. The preservation of variable amounts of brine assimilation in a preeruptive basaltic melt is considered unlikely. There is no petrographic evidence of magma mixing being preserved within this sample. Consistent K/Cl and Br/Cl across sections #3 to #7 further indicates that the original melt had a consistent geochemical signature and magma mixing did not produce the geochemical variability in the glass sections. Variations in concentration can be attributed to the heterogeneous nature of the sample, which contains variable amounts of glass, microcrystalline matrix and fully crystalline phases. Halogens and K are concentrated in the glass and microcrystalline matrix compared to the crystalline phases and heterogeneous sampling during bulk analysis will lead to varying concentrations across the sample without altering the K/Cl and Br/Cl ratios [*Foland et al*., 1993]. The low K/Cl and Br/Cl in sections #1 and #2 compared to the inner sections cannot therefore have been produced be either mixing of two different magma sources, or the heterogeneous assimilation and preservation of brine within the magma chamber and must have been introduced during or after eruption when sample homogenization was no longer possible.

Submarine lava flows have been shown to feature cavities indicative of vapor being present during eruption [*Perfit et al*., 2003; *Soule et al*., 2006]. The vapor is formed from the phase separation of seawater, trapped within the lava. Chemical interaction between the vapor and the still molten lava is limited, although the brine phase may become trapped in the lava leading to heterogeneous Cl contamination is the areas surrounding the trapped brine [*Portner et al*., 2014; *Soule et al*., 2006]. The eruption of basalt DR25A1b at magmatic temperatures and at pressures of 43 Mbar directly into seawater would result in the phase separation

Table 2. Quantification of Brine Assimilation for Sections #1 and #2

Section No.	Ratio Used[a]	Measured[b] Cl (ppm)	Calculated[c] Cl %	Calculated[c] Cl (ppm)
#1	K/Cl	28.12 ± 0.70	48.8 ± 0.7	13.5–13.9
	H_2O/Cl	28.12 ± 0.70	44.5 ± 17.0	7.8–17.2
	Br/Cl	28.12 ± 0.70	27.8 ± 5.1	6.4–9.2
#2	K/Cl	66.08 ± 0.07	81.6 ± 0.4	53.7–54.2
	H_2O/Cl	66.08 ± 0.07	>70.3	> 46.5
	Br/Cl	66.08 ± 0.07	81.9 ± 3.3	51.7–56.0

[a]Refers to the elemental ratios (K/Cl, H_2O/Cl, and Br/Cl used within equation (1) to determine the percentage of assimilated Cl.
[b]Chlorine concentrations measured within glass chips #1 and #2 assumed to contain an assimilated brine component.
[c]Percentage of assimilated Cl is calculated from equation (1), with Cl concentration derived from assimilation also shown.

of any trapped seawater into a brine and vapor phase within the NaCl-H_2O system [*Driesner and Heinrich*, 2007]. The H_2O/Cl and Br/Cl within sections #1 and #2 may therefore be the result the rapid assimilation of brines originating from seawater into the melt or recently cooled glass during eruption, leading to heterogeneous assimilation within the glass margin.

6.3. Quantifying Brine Assimilation

If it is assumed that the Cl, Br, K, and H_2O are only being added by the assimilation of a brine component and that contributions from the possible (microbial) alteration of section #1 discussed earlier is minor, then it is possible to estimate the quantity of brine derived Cl added to sections #1 and #2 [*Kendrick et al.*, 2013]:

$$\%\ \text{Assimilated Cl} = 1 - \frac{\left[\frac{X}{Cl}\ \text{assimilant} - \frac{X}{Cl}\text{glass}\right]}{\left[\frac{X}{Cl}\ \text{assimilant} - \frac{X}{Cl}\text{melt}\right]} \times 100 \quad (1)$$

where X = Br, K, and H_2O, enables the percentage of assimilated Cl within the glass to be calculated. The X/Cl values of the melt are estimated by averaging values obtained from sections #3 to #7 yielding K/Cl = 39.8 ± 0.4; Br/Cl = 1.33 ± 0.07 ($\times 10^{-3}$); and H_2O/Cl = 92.5 ± 9.7. Appropriate X/Cl for sections #1 and #2 are used for the glass compositions in equation (1). For simplicity, we assume the K/Cl value of the assimilant to be low at 0.1 ± 0.09, determined from the direct measurement of hydrothermal brines [*Böhlke and Irwin*, 1992; *Thompson and Fournier*, 1988]. The Br/Cl (1.83 ± 0.30 $\times 10^{-4}$) and the H_2O/Cl (17.84 ± 16.33) ratios for the assimilant are calculated previously using error-weighted regressions to limit the influence of data with large errors.

The amount of assimilation within sections #1 and #2 is summarized in Table 2. All estimates calculated using the extrapolated ratios (Br/Cl and H_2O/Cl) in equation (1) take into account the errors associated with the regression, and values stated in Table 2 show the maximum possible range of assimilated Cl. Section #2 which is the most affected, is estimated to have derived greater than 70% of its total Cl content from assimilation of a brine component. The percentage of Cl assimilated in section #2, using K/Cl and Br/Cl produces similar estimates of 81.6 ± 0.3% and 81.9 ± 3.3%, respectively. The proportion based on H_2O/Cl is broadly consistent at 91.5 ± 21.1%. Estimates of Cl assimilation in section #1 are similar using K/Cl (48.8 ± 0.7%) and the H_2O/Cl (44.5 ± 17.0%); however Br/Cl gives a slightly lower value (27.8 ± 5.1%). As the calculation assumes any deviation from the average melt value is due to addition from the assimilant and not due to sample heterogeneity or other forms of contamination, the proportion of brine assimilation calculated for sections #1 and #2 is considered to represent an upper limit.

6.4. Assimilation Mechanism

Within the limitations of the calculation, section #2 appears to contain the highest proportion of brine component. The greater amount of brine assimilation calculated in section #2 requires there to be a process which can introduce or maintain brine/melt interaction heterogeneously throughout the glass margin.

Petrographically there is no evidence for assimilation in section #2 (supporting information), however higher Cl and Na content within glasses along the edges of the visible fractures and surrounding vesicles of trapped seawater compared with fracture and vesicle free glass indicates that seawater can be introduced and interact with the basaltic melt locally [*Schiffman et al.*, 2010; *Soule et al.*, 2006].

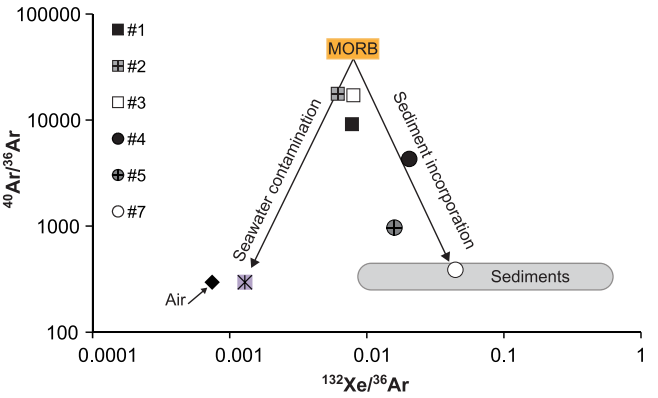

Figure 7. Adaptation of Figure 4 from *Kumagai and Kaneoka* [1998] showing the $^{132}Xe/^{36}Ar$ versus $^{40}Ar/^{36}Ar$ of all sections (excluding #6) as well as new $^{40}Ar/^{36}Ar$ from sections #2 and #4 from this study. The sections are displayed against the MORB [*Graham*, 2002] and possible contamination end-members, including air, seawater [*Ozima and Podosek*, 1983], and sediments [*Matsuda and Nagao*, 1986]. The ratios from the samples show that the ratios from the deep glass (#2 and #3) have the lowest degree of contamination and have mostly retained their original MORB signature. Other sections have experienced contamination with samples trending toward atmospheric $^{40}Ar/^{36}Ar$ and greater than atmospheric $^{132}Xe/^{36}Ar$ similar to oceanic sediments. Errors are smaller than symbols.

Section #1, which was in direct contact with the surrounding seawater during eruption, would have experienced rapid quenching [*Griffiths and Fink*, 1992] and as such would have been closed to any interaction with the seawater relatively quickly. The inner sections of the quenched margin would then have been insulated from the cooling seawater by the quenched outer glass and therefore would have remained molten for a longer period of time allowing the inner sections to continue interacting with the brine phase. Concentrations gradients of Cl, Na, and K across fractures in submarine basaltic glass are consistent with diffusion between seawater-derived fluids and the glass while still molten or at temperatures within the glass transition interval [*Schiffman et al.*, 2010]. Areas of Cl enrichment surrounding these fractures exhibit a reddening of the glass due to the rapid oxidation of ferrous iron in melt in response to seawater interaction (Figure 8). Section #1 also exhibits a red alteration along the surface of the glass margin and within fractures, suggesting that these fractures may act as a conduit for the introduction of seawater into the deeper glass (Figure 2).

The encapsulation of seawater in the melt is another process which may have introduced a brine component into the glass. Large vesicles (1–5 mm) in the surface of the glass are thought to be formed from seawater being trapped as the surface deforms and folds, which can enrich the surrounding glass by up to an order of magnitude relative to the ambient glass concentration [*Soule et al.*, 2006]. No evidence of seawater

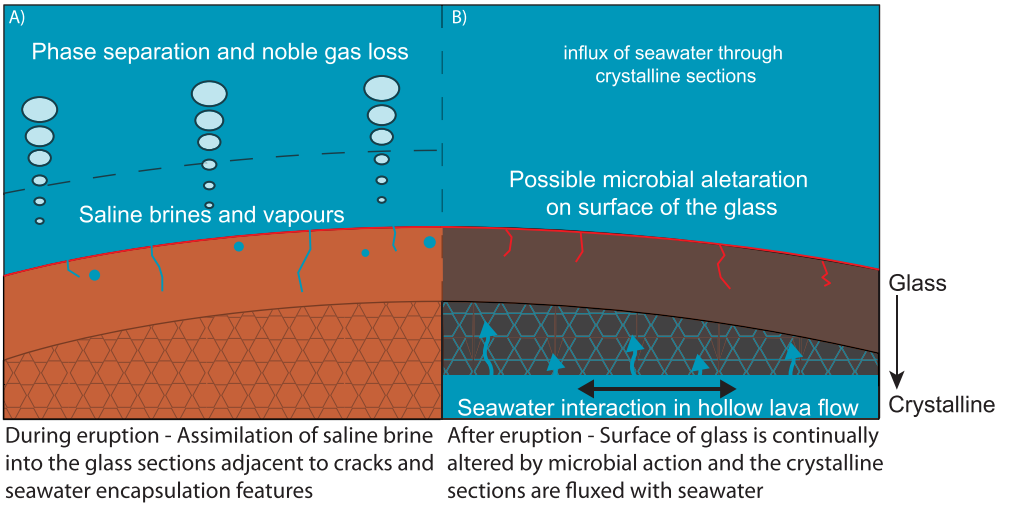

Figure 8. Conceptual model of seawater contamination within a deep sea basaltic lava margin during and after eruption. (a) During the eruption the outer glass sections incorporate a saline brine component, formed by the hydrothermal boiling of the surrounding seawater. Phase separation during boiling leads to halogen fractionation and loss of seawater-derived noble gases; the resulting saline brine is then incorporated into the glass along cracks or within seawater encapsulation features. The interaction between the molten glass and seawater causes rapid oxidation of the glass leading to reddening of the glass on the outer glass surface and along fractures. (b) The surface of the glass rim shows an enrichment in iodine from the possible microbial alteration of the glass in continuous contact with seawater. The crystalline interior has atmospheric $^{40}Ar/^{36}Ar$ and greater than atmosheric $^{132}Xe/^{36}Ar$ most likely introduced through the interaction of seawater with the crystalline sections leading to noble gas adsorption and potential heavy element enrichment.

encapsulation features are seen within sections #1 and #2 of the chilled margin although the limited sample size does not rule out seawater encapsulation as a potential mechanism for the introduction of the brines in to basaltic glass margins.

The mechanism for the heterogeneous introduction of brine into the glass of this sample is ultimately unknown. However, evidence of fractures with reddened edges of the glass section #1, which are thought to represent seawater/melt interaction, is one possible mechanism for the heterogeneous assimilation throughout the glass. Section #2, which is calculated to be the most contaminated shows little evidence for fractures with reddened, or Cl enriched edges (Figures 2 and 8). The lack of petrographic evidence for possible assimilation features in section #2 does not rule out the possibility of brine assimilation but only concludes that even detailed petrography may not be able to identify all areas of contamination within basaltic glass samples especially if it is heterogeneously distributed and on a small-scale limiting the detection of Cl enriched zones.

6.5. Sedimentary Uptake?

Noble gas ratios from within the sections have previously been suggested to contain a sedimentary component [*Kumagai and Kaneoka*, 1998]. The $^{40}Ar/^{36}Ar$ and $^{132}Xe/^{36}Ar$ ratios of all crystalline sections lie along a mixing line defined by the mixing of a MORB component with that of a sedimentary end-member toward the sample interior, with section #7 indistinguishable from the sedimentary ratio (Figure 7). This was explained previously by incorporation of fine-grained sediment disturbed and incorporated into the molten interior [*Kumagai and Kaneoka*, 1998]. Iodine is particularly enriched in organic-rich sediments due to the biophillic behavior of this element [*Muramatsu et al*., 2001]. The I/Cl ratios of interior sections with sedimentary $^{40}Ar/^{36}Ar$ and $^{132}Xe/^{36}Ar$ ratios, range from MORB-like to slightly elevated I/Cl ratios but show no progression toward more sedimentary-like values toward the interior, with the glass section #1 having the highest I/Cl of any section (Figure 5).

The basaltic chilled margin used in this study originates from the neovolcanic zone of the RTJ, which typically has little sediment; the direct incorporation of sediment into the erupting melt is therefore thought to be unlikely [*Kumagai and Kaneoka*, 2005]. The entire sample represents the chilled margin of a drained basaltic lava flow [*Kumagai and Kaneoka*, 2003, 2005]. The hollow lava flow would have allowed seawater to interact with the crystalline interior. The posteruption infiltration of seawater along the grain boundaries of the inner sections could cause noble gases to be adsorbed to the grain surface. The adsorption of noble gases can cause mass fractionation and enrichment in heavier elements (Xe > Kr > Ar), which is a contributing factor to the Xe enrichment in sediments [*Fanale and Cannon*, 1971].

The flux of seawater through the hollow lava flow could also introduce I into the crystalline interior through microbial alteration which is suggested to be the cause of the high I concentration and I/Cl ratio in section #1. A similar process may control the I concentration within section #7, although there is little evidence that microbial alteration within crystalline basalt is pervasive compared to basaltic glass [*Torsvik et al*., 1998]. The enrichment of I in the section #1 and #7 as well as Xe in section #7 is most likely not related to the physical incorporation of sediments into the melt as previously suggested and is more likely due to another process or combination of processes such as heavy element enrichment from adsorption and, or microbial alteration.

6.6. Implications

Contamination within the quenched margin of sample DR25A1b is heterogeneously distributed within the outer glass sections, with no correlation between distance from the sample surface/seawater interface and the degree of contamination. Section #2 has a geochemical signature that requires that it to have assimilated a Cl-rich brine component however, there is no petrographic evidence of alteration or Cl bearing secondary minerals being present in this section (Figure 2 and supporting information Figure S2). Detailed petrography only provides a two-dimensional snapshot of any given sample and therefore even detailed petrography may not be able to identify basaltic glass samples which contain an assimilated component.

The level of contamination in this sample is significant, although the unique Br/Cl and I/Cl signatures within the outer glass sections are not prevalent in previous studies of halogens in submarine basalts [*Kendrick et al*., 2012b, 2013]. The low starting halogen concentrations in this sample, which is typical of N-MORB type basalts may be a factor in the degree of contamination, with a small degree of assimilation being able to

overprint the original halogen signature. The mechanism of assimilation is ultimately unknown and further investigation is needed to establish whether fractures play a role as conduits for introducing hydrothermal fluids to the glass interior and if N-MORB are more susceptible to this type of localized contamination. Until the exact mechanism of assimilation is known it is recommended to avoid heavily fractured glass and select multiple chips from the same sample or samples with a wider spatial sample distribution originating from the same eruption to limit the contribution from any localized contamination that may be present as shown in this study.

Br/Cl and I/Cl variation in submarine basalts considered to be free from contamination is, 1–2 $\times$ 10^{-3} and 1–5 $\times$ 10^{-5}, respectively. Previous research has indicated that samples out-with these ranges have assimilated a Cl-rich brine component into the melt, with up to 95% of the Cl within the samples being derived from assimilation [*Kendrick et al*., 2013]. Our study has shown that this level of Cl assimilation (up to 70%) can occur at a small-scale within submarine basalts, through direct interaction with seawater during eruption, without showing obvious contamination indicators. The Br/Cl and I/Cl variance observed in the mantle from the analysis of visually and petrographically uncontaminated submarine basalt samples therefore may not be representative of the mantle as small-scale assimilation in submarine basalt samples may be a contributing factor to the heterogeneity observed. The mantle Br/Cl and I/Cl may therefore be even more homogeneous than currently thought.

Finally, the degree of halogen assimilation within sections #1 and #2 as estimated from the halogen, K and H_2O data is not consistent with evidence from the noble gases. Section #2 contains the highest proportion of assimilated brine; however, this sample has a mantle-like $^{40}Ar/^{36}Ar$ ratio, similar to the value of the least brine-affected glass section (#3). Halogen and noble gas contamination within the contaminated sections therefore appears decoupled with brine assimilation not appearing to introduce a significant atmospheric noble gas component perhaps due to significant amount of noble gas loss ($\sim$30%) from brines during phase separation [*Winckler et al*., 2000]. Noble gas contamination within the glass sections is therefore most likely a secondary feature added during sample handling, which can therefore be mitigated against by using steps such as using multiple step heating analysis or storing sample under vacuum prior to analysis [*Ballentine and Barfod*, 2000; *Kumagai and Kaneoka*, 2003].

7. Conclusion

Geochemical evidence from halogen, K, H_2O, and noble gas data indicates that the outer glass layers of quenched submarine MORB can be contaminated through the direct interaction with surrounding seawater during eruption.

The assimilant found to be present within the glass margin is not that of pure seawater but a saline brine phase. This is formed by boiling and phase separation of seawater during the eruption of the lava. The boiling and phase separation of seawater also partitions the noble gases into the vapor phase, and will therefore have a limited effect on the noble gas signature of the sample.

The level of contamination estimated within the glass rind can be significant with up to $\sim$70% of the Cl being derived from assimilation, suggesting that under certain conditions small amounts of brine assimilation during eruption can significantly overprint the original halogen signature. The assimilated component appears to be heterogeneously distributed throughout the glass and may be related to the location of fractures within the glass.

This study shows that interactions between an erupting basaltic lava flow and the surrounding seawater has the potential to overprint the original halogen mantle signature at a level that is similar to the range of variance found in the accepted range of uncontaminated erupted MORB. Future studies that deal with marine overprinting of glass samples will be required to reflect on whether this variance is eruption related or represents real variance in the MORB-source.

Acknowledgments
We would like to thank J. Cowpe, D. Blagburn, and B. Clementson for the technical support with the mass spectrometers and K. H. Joy and J. Fellowes for their help with petrography and the use of the ESEM. We gratefully acknowledge the constructive reviews from Matthew Loewen, Froukje M. van der Zwan, and two anonymous reviewers that significantly improved the manuscript. The sample used in this study was originally distributed through an on-board scientist of the R/V Hakuho Maru (cruise KH93–3), T. Fujii of Univ. Tokyo. This study was carried out under an agreement to distribute the sample to the authors by the members of the KH93–3 cruise on-board scientists. Data generated from this study are presented in Table 1; any additional data may be obtained from MWB (broadley@crpg.cnrs-nancy.fr). This work was financially supported though a NERC studentship NE/J500057/1 (to M. W. B.) and ERC-267692 NOBLE grant (C. J. B. and R. B.).

References

Ballentine, C. J., and D. N. Barfod (2000), The origin of air-like noble gases in MORB and OIB, *Earth Planet. Sci. Lett.*, *180*(1), 39–48.
Berndt, M. E., and W. E. Seyfried Jr. (1990), Boron, bromine, and other trace elements as clues to the fate of chlorine in mid-ocean ridge vent fluids, *Geochim. Cosmochim. Acta*, *54*(8), 2235–2245.

Berndt, M. E., and W. E. Seyfried Jr. (1997), Calibration of BrCl fractionation during subcritical phase separation of seawater: Possible halite at 9 to 10°N East Pacific Rise, *Geochim. Cosmochim. Acta*, *61*(14), 2849–2854.
Böhlke, J., and J. Irwin (1992), Laser microprobe analyses of Cl, Br, I, and K in fluid inclusions: Implications for sources of salinity in some ancient hydrothermal fluids, *Geochim. Cosmochim. Acta*, *56*(1), 203–225.
Bonifacie, M., N. Jendrzejewski, P. Agrinier, E. Humler, M. Coleman, and M. Javoy (2008), The chlorine isotope composition of Earth's mantle, *Science*, *319*(5869), 1518–1520.
Broadley, M. W., C. J. Ballentine, D. Chavrit, L. Dallai, and R. Burgess (2016), Sedimentary halogens and noble gases within Western Antarctic xenoliths: Implications of extensive volatile recycling to the sub continental lithospheric mantle, *Geochim. Cosmochim. Acta*, *176*, 139–156.
Burgess, R., E. Layzelle, G. Turner, and J. Harris (2002), Constraints on the age and halogen composition of mantle fluids in Siberian coated diamonds, *Earth Planet. Sci. Lett.*, *197*(3), 193–203.
Burnard, P., D. Graham, and K. Farley (2004), Fractionation of noble gases (He, Ar) during MORB mantle melting: A case study on the Southeast Indian Ridge, *Earth Planet. Sci. Lett.*, *227*(3–4), 457–472.
Burnard, P. G., F. M. Stuart, G. Turner, and N. Oskarsson (1994), Air contamination of basaltic magmas: Implications for high $^{3}He/^{4}He$ mantle Ar isotopic composition, *J. Geophys. Res.*, *99*(B9), 17,709–17,715.
Butterfield, D. A., R. E. McDuff, M. J. Mottl, M. D. Lilley, J. E. Lupton, and G. J. Massoth (1994), Gradients in the composition of hydrothermal fluids from the Endeavour segment vent field: Phase separation and brine loss, *J. Geophys. Res.*, *99*(B5), 9561–9583.
Chavrit, D., R. Burgess, H. Sumino, D. A. Teagle, G. Droop, A. Shimizu, and C. J. Ballentine (2016), The contribution of hydrothermally altered ocean crust to the mantle halogen and noble gas cycles, *Geochim. Cosmochim. Acta*, *183*, 106–124.
Crowell, B. W., R. P. Lowell, and K. L. Von Damm (2008), A model for the production of sulfur floc and "snowblower" events at mid-ocean ridges, *Geochem. Geophys. Geosyst.*, *9*, Q10T02, doi:10.1029/2008GC002103.
Deruelle, B., G. Dreibus, and A. Jambon (1992), Iodine abundances in oceanic basalts: Implications for Earth dynamics, *Earth Planet. Sci. Lett.*, *108*(4), 217–227.
Driesner, T., and C. A. Heinrich (2007), The system H_2O–NaCl. Part I: Correlation formulae for phase relations in temperature-pressure-composition space from 0 to 1000°C, 0 to 5000bar, and 0 to 1 X NaCl, *Geochim. Cosmochim. Acta*, *71*(20), 4880–4901.
Fanale, F. P., and W. A. Cannon (1971), Physical adsorption of rare gas on terrigenous sediments, *Earth Planet. Sci. Lett.*, *11*(1–5), 362–368.
Fehn, U., G. Snyder, and P. K. Egeberg (2000), Dating of pore waters with ^{129}I: Relevance for the origin of marine gas hydrates, *Science*, *289*(5488), 2332–2335.
Fehn, U., G. T. Snyder, R. Matsumoto, Y. Muramatsu, and H. Tomaru (2003), Iodine dating of pore waters associated with gas hydrates in the Nankai area, Japan, *Geology*, *31*(6), 521–524.
Fehn, U., G. Snyder, and Y. Muramatsu (2007), Iodine as a tracer of organic material: ^{129}I results from gas hydrate systems and fore arc fluids, *J. Geochem. Explor.*, *95*(1), 66–80.
Foland, K. A., T. H. Fleming, A. Heimann, and D. H. Elliot (1993), Potassium-argon dating of fine-grained basalts with massive Ar loss: Application of the 40Ar39Ar technique to plagioclase and glass from the Kirkpatrick Basalt, Antarctica, *Chem. Geol.*, *107*(1–2), 173–190.
Foustoukos, D. I., and W. E. Seyfried Jr. (2007), Trace element partitioning between vapor, brine and halite under extreme phase separation conditions, *Geochim. Cosmochim. Acta*, *71*(8), 2056–2071.
Graham, D. W. (2002), Noble gas isotope geochemistry of mid-ocean ridge and ocean island basalts: Characterization of mantle source reservoirs, *Rev. Mineral. Geochem.*, *47*(1), 247–317.
Griffiths, R. W., and J. H. Fink (1992), Solidification and morphology of submarine lavas: A dependence on extrusion rate, *J. Geophys. Res.*, *97*(B13), 19,729–19,737.
Holland, G., and C. J. Ballentine (2006), Seawater subduction controls the heavy noble gas composition of the mantle, *Nature*, *441*(7090), 186–191.
Jambon, A., B. Déruelle, G. Dreibus, and F. Pineau (1995), Chlorine and bromine abundance in MORB: The contrasting behaviour of the Mid-Atlantic Ridge and East Pacific Rise and implications for chlorine geodynamic cycle, *Chem. Geol.*, *126*(2), 101–117.
Johnson, L., R. Burgess, G. Turner, H. Milledge, and J. Harris (2000), Noble gas and halogen geochemistry of mantle fluids: Comparison of African and Canadian diamonds, *Geochim. Cosmochim. Acta*, *64*(4), 717–732.
Kastner, M., H. Elderfield, J. B. Martin, E. Suess, K. A. Kvenvolden, and R. E. Garrison (1990), Diagenesis and interstitial-water chemistry at the Peruvian continental margin—Major constituents and strontium isotopes, *Proc. Ocean Drill. Program Sci. Resul.*, *112*, 413–440.
Kendrick, M. A. (2012), High precision Cl, Br and I determinations in mineral standards using the noble gas method, *Chem. Geol.*, *292*, 116–126.
Kendrick, M. A., and P. Burnard (2013), Noble gases and halogens in fluid inclusions: A journey through the Earth's crust, in *The Noble Gases as Geochemical Tracers*, edited by P. Burnard, pp. 319–369, Springer, Berlin.
Kendrick, M. A., J. D. Woodhead, and V. S. Kamenetsky (2012a), Tracking halogens through the subduction cycle, *Geology*, *40*(12), 1075–1078.
Kendrick, M. A., V. S. Kamenetsky, D. Phillips, and M. Honda (2012b), Halogen systematics (Cl, Br, I) in mid-ocean ridge basalts: A Macquarie Island case study, *Geochim. Cosmochim. Acta*, *81*, 82–93.
Kendrick, M. A., R. Arculus, P. Burnard, and M. Honda (2013), Quantifying brine assimilation by submarine magmas: Examples from the Galápagos Spreading Centre and Lau Basin, *Geochim. Cosmochim. Acta*, *123*, 150–165.
Kent, A. J. R., D. A. Clague, M. Honda, E. M. Stolper, I. D. Hutcheon, and M. D. Norman (1999), Widespread assimilation of a seawater-derived component at Loihi Seamount, Hawaii, *Geochim. Cosmochim. Acta*, *63*(18), 2749–2761.
Kent, A. J., D. W. Peate, S. Newman, E. M. Stolper, and J. A. Pearce (2002) Chlorine in submarine glasses from the Lau Basin: Seawater contamination and constraints on the composition of slab-derived fluids, *Earth Planet. Sci. Lett.*, *202*(2), 361–377.
Kumagai, H., and I. Kaneoka (1998), Variations of noble gas abundances and isotope ratios in a single MORB pillow, *Geophys. Res. Lett.*, *25*(20), 3891–3894.
Kumagai, H., and I. Kaneoka (2003), Relationship between submarine MORB glass textures and atmospheric component of MORBs, *Chem. Geol.*, *200*(1–2), 1–24.
Kumagai, H., and I. Kaneoka (2005), Noble gas signatures around the Rodriguez Triple Junction in the Indian Ocean: Constraints on magma genesis in a ridge system, *Geochim. Cosmochim. Acta*, *69*(23), 5567–5583.
Kyser, T. K., and J. R. O'Neil (1984), Hydrogen isotope systematics of submarine basalts, *Geochim. Cosmochim. Acta*, *48*(10), 2123–2133.
le Roux, P. J., S. B. Shirey, E. H. Hauri, M. R. Perfit, and J. F. Bender (2006), The effects of variable sources, processes and contaminants on the composition of northern EPR MORB (8–10°N and 12–14°N): Evidence from volatiles (H_2O, CO_2, S) and halogens (F, Cl), *Earth Planet. Sci. Lett.*, *251*, 209–231.

Liebscher, A., V. Lüders, W. Heinrich, and G. Schettler (2006), Br/Cl signature of hydrothermal fluids: Liquid-vapour fractionation of bromine revisited, *Geofluids*, *6*(2), 113–121.
Martin, J. B., J. M. Gieskes, M. Torres, and M. Kastner (1993), Bromine and iodine in Peru margin sediments and pore fluids: Implications for fluid origins, *Geochim. Cosmochim. Acta*, *57*(18), 4377–4389.
Matsuda, J.-I., and K. Nagao (1986), Noble gas abundances in a deep-sea sediment core from eastern equatorial Pacific, *Geochem. J.*, *20*(2), 71–80.
Merrihue, C., and G. Turner (1966), Potassium-argon dating by activation with fast neutrons, *J. Geophys. Res.*, *71*(11), 2852–2857.
Michael, P. J., and J. G. Schilling (1989), Chlorine in mid-ocean ridge magmas: Evidence for assimilation of seawater-influenced components, *Geochim. Cosmochim Acta*, *53*(12), 3131–3143.
Michael, P. J., and W. C. Cornell (1998), Influence of spreading rate and magma supply on crystallization and assimilation beneath mid-ocean ridges: Evidence from chlorine and major element chemistry of mid-ocean ridge basalts, *J. Geophys. Res.*, *103*(B8), 18,325–18,356.
Michael, P. J., C. H. Langmuir, H. J. B. Dick, J. E. Snow, S. L. Goldstein, D. W. Graham, and H. N. Edmonds (2003), Magmatic and amagmatic seafloor generation at the ultraslow-spreading Gakkel ridge, Arctic Ocean, *Nature*, *423*(6943), 956–961.
Michard, A., R. Montigny, and R. Schlich (1986), Geochemistry of the mantle beneath the Rodriguez Triple Junction and the South-East Indian Ridge, *Earth Planet. Sci. Lett.*, *78*(1), 104–114.
Mukhopadhyay, S. (2012), Early differentiation and volatile accretion recorded in deep-mantle neon and xenon, *Nature*, *486*(7401), 101–104.
Muramatsu, Y., U. Fehn, and S. Yoshida (2001), Recycling of iodine in fore-arc areas: Evidence from the iodine brines in Chiba, Japan, *Earth Planet. Sci. Lett.*, *192*(4), 583–593.
Muramatsu, Y., T. Doi, H. Tomaru, U. Fehn, R. Takeuchi, and R. Matsumoto (2007), Halogen concentrations in pore waters and sediments of the Nankai Trough, Japan: Implications for the origin of gas hydrates, *Appl. Geochem.*, *22*(3), 534–556.
Nakamura, K., Y. Kato, K. Tamaki, and T. Ishii (2007), Geochemistry of hydrothermally altered basaltic rocks from the Southwest Indian Ridge near the Rodriguez Triple Junction, *Mar. Geol.*, *239*(3), 125–141.
Oosting, S. E., and K. L. Von Damm (1996), Bromide/chloride fractionation in seafloor hydrothermal fluids from 9–10°N East Pacific Rise, *Earth Planet. Sci. Lett.*, *144*(1–2), 133–145.
Ozima, M., and F. A. Podosek (2002), *Noble Gas Geochemistry*, Cambridge Univ. Press, Cambridge, U. K.
Patterson, D., M. Honda, and I. McDougall (1990), Atmospheric contamination: A possible source for heavy noble gases in basalts from Loihi seamount, Hawaii, *Geophys. Res. Lett.*, *17*(6), 705–708.
Parai, R., S. Mukhopadhyay, and J. J. Standish (2012), Heterogeneous upper mantle Ne, Ar and Xe isotopic compositions and a possible Dupal noble gas signature recorded in basalts from the Southwest Indian Ridge, *Earth Planet. Sci. Lett.*, *359–360*, 227–239.
Patterson, D., M. Honda, and I. McDougall (1990), Atmospheric contamination: A possible source for heavy noble gases in basalts from Loihi seamount, Hawaii, *Geophys. Res. Lett.*, *17*(6), 705–708.
Pepin, R. O., and D. Porcelli (2002), Origin of noble gases in the terrestrial planets, *Rev. Mineral. Geochem.*, *47*(1), 191–246.
Perfit, M. R., J. R. Cann, D. J. Fornari, J. Engels, D. K. Smith, W. I. Ridley, and M. H. Edwards (2003), Interaction of sea water and lava during submarineeruptions at mid-ocean ridges, *Nature*, *426*(6962), 62–65.
Pietruszka, A. J., M. D. Norman, M. O. Garcia, J. P. Marske, and D. H. Burns (2013), Chemical heterogeneity in the Hawaiian mantle plume from the alteration and dehydration of recycled oceanic crust, *Earth Planet. Sci. Lett.*, *361*, 298–309.
Portner, R. A., D. A. Clague, and J. B. Paduan (2014), Caldera formation and varied eruption styles on North Pacific seamounts: The clastic lithofacies record, *Bull. Volcanol.*, *76*(8), 845.
Price, R. C., A. K. Kennedy, M. Riggs-Sneeringer, and F. A. Frey (1986), Geochemistry of basalts from the Indian Ocean triple junction: Implications for the generation and evolution of Indian Ocean ridge basalts, *Earth Planet. Sci. Lett.*, *78*(4), 379–396.
Ruzié-Hamilton, L., P. Clay, R. Burgess, B. Joachim, C. J. Ballentine, and G. Turner (2016), Determination of halogen abundances in terrestrial and extraterrestrial samples by the analysis of noble gases produced by neutron irradiation, *Chem. Geol.*, *437*, 77–87.
Saal, A. E., E. H. Hauri, C. H. Langmuir and M. R. Perfit (2002), Vapour undersaturation in primitive mid-ocean-ridge basalt and the volatile content of Earth's upper mantle, *Nature*, *419*, 451–455.
Schiffman, P., R. Zierenberg, W. W. Chadwick, D. A. Clague, and J. Lowenstern (2010), Contamination of basaltic lava by seawater: Evidence found in a lava pillar from Axial Seamount, Juan de Fuca Ridge, *Geochem. Geophys. Geosyst.*, *11*, Q04004, doi:10.1029/2009GC003009.
Schilling, J. G., C. K. Unni, and M. L. Bender (1978), Origin of chlorine and bromine in the oceans, *Nature*, *273*(5664), 631–636.
Schilling, J.-G., M. Bergeron, R. Evans, and J. Smith (1980), Halogens in the mantle beneath the North Atlantic [and discussion], *Philos. Trans. R. Soc. A*, *297*(1431), 147–178.
Soule, S. A., D. J. Fornari, M. R. Perfit, W. I. Ridley, M. H. Reed, and J. R. Cann (2006), Incorporation of seawater into mid-ocean ridge lava flows during emplacement, *Earth Planet. Sci. Lett.*, *252*(3), 289–307.
Stoessell, R. K., and A. B. Carpenter (1986), Stoichiometric saturation tests of $NaCl_{1-x}Br_x$ and $KCl_{1-x}Br_x$, *Geochim. Cosmochim. Acta*, *50*(7), 1465–1474.
Stroncik, N. A., and H. U. Schmincke (2002), Palagonite—A review, *Int. J. Earth Sci.*, *91*(4), 680–697.
Sumino, H., R. Burgess, T. Mizukami, S. R. Wallis, G. Holland, and C. J. Ballentine (2010), Seawater-derived noble gases and halogens preserved in exhumed mantle wedge peridotite, *Earth Planet. Sci. Lett.*, *294*(1), 163–172.
Templeton, A. S., H. Staudigel, and B. M. Tebo (2005), Diverse Mn (II)-oxidizing bacteria isolated from submarine basalts at Loihi Seamount, *Geomicrobiol. J.*, *22*(3–4), 127–139.
Thompson, J. M., and R. O. Fournier (1988), Chemistry and geothermometry of brine produced from the Salton Sea Scientific Drill Hole, Imperial Valley, California, *J. Geophys. Res.*, *93*(B11), 13,165–13,173.
Torsvik, T., H. Furnes, K. Muehlenbachs, I. H. Thorseth, and O. Tumyr (1998), Evidence for microbial activity at the glass-alteration interface in oceanic basalts, *Earth Planet. Sci. Lett.*, *162*(1), 165–176.
van der Zwan, F. M., C. W. Devey, N. Augustin, R. R. Almeev, R. A. Bantan, and A. Basaham (2015), Hydrothermal activity at the ultraslow- to slow-spreading Red Sea Rift traced by chlorine in basalt, *Chem. Geol.*, *405*(5), 63–81.
Winckler, G., R. Kipfer, W. Aeschbach-Hertig, R. Botz, M. Schmidt, S. Schuler, and R. Bayer (2000), Sub sea floor boiling of Red Sea brines: New indication from noble gas data, *Geochim. Cosmochim. Acta*, *64*(9), 1567–1575.